Surface Review and Letters, Vol. 17, No. 2 (2010) 215–221

DOI: 10.1142/S0218625X10013886

World Scientific
www.worldscientific.com

REACTIVE HOT PRESSING AND OXIDATION BEHAVIOR OF Hf-BASED ULTRA-HIGH-TEMPERATURE CERAMICS

SEUNG JUN LEE*, EUL SON KANG†, SEUNG SU BAEK†
and DO KYUNG KIM*,‡
*Department of Materials Science and Engineering,
Korea Advanced Institute of Science and Technology (KAIST),
335 Gwahangno, Yuseong-gu, Daejeon 305-701, Republic of Korea
†Agency for Defense Development (ADD),
462 Jochiwongil, Yuseong-gu, Daejeon 305-600, Republic of Korea
‡dkkim@kaist.ac.kr

Received 21 January 2009

A HfB_2-SiC ceramics were fabricated via a reactive hot pressing using Hf, B_4C, and Si as precursors. The reaction temperature for the reactive hot pressing between 1800 and 1900°C was determined by reaction of the precursor at different temperatures from 900 to 1800°C. The effective size reduction of precursors was investigated by vibration milling, which exhibited a critical role to achieve high densification and uniform microstructure. Also, it has affected the oxidation behavior of HfB_2–SiC in air. Vibration milled sample showed uniform surface of SiO_2 layer, but sample which was fabricated by as-received powder exhibited non-uniform oxidation behavior. Examination of the mechanical properties showed that particle size reduction via vibration also led to improved flexural strength, hardness and fracture toughness.

Keywords: Reactive hot pressing; boride; vibration milling; oxidation.

1. Introduction

Transition-metal borides have gained considerable importance as ultra-high-temperature ceramics (UHTCs) because of their advantageous characteristic of melting points >3000°C, oxidation resistance and thermal shock resistance.[1,2] UHTCs have been extensively investigated for high temperature structural applications that include thermal protection materials for atmospheric re-entry, hypersonic flight, and rocket propulsion. UHTCs materials, such as zirconium diboride (ZrB_2) and hafnium diboride (HfB_2) exposed to air below 1100°C undergo oxidation to HfO_2 and B_2O_3 (l). And the addition of SiC in matrices of ZrB_2 and HfB_2 improved the oxidation resistance by forming an SiO_2 layer on the surface up to 1700°C.[3,4]

Transition-metal borides typically need relatively high temperature (>1900°C) and high pressure (>30 MPa) to obtain dense samples because of strong covalent bonding and low diffusion coefficient.[2] Therefore, metallic additives have been used to promote liquid-phase formation that can reduce densification temperature, but it can deteriorate the high temperature properties.[5] Recently, pressureless sintering of transition-metal borides has been widely investigated by using WC, B_4C, C,

‡Corresponding author.

and $MoSi_2$.[6–8] In contrast to sintering aid assisted sintering methods, spark plasma sintering (SPS) has been reported to possess advantages, such as fast heating rate, short sintering time, high density, and clean grain boundaries.[9] Another alternative advantageous method is reactive hot pressing (RHP), which involves both the synthesis and densification into single-step process leading to high density ceramics at reduced temperatures, and lower impurity contents compared with conventional process.[10,11] Many reports stated that microstructure of the material fabricated by reactive hot pressing is strongly co-related with particle size of the precursor powder. The present work reports on the fabrication of HfB_2–SiC composite via a RHP technique. The composite fabrication temperature range was investigated by reaction of the precursor at different temperatures from 900 to 1800°C. Also, effects of precursor powder on the densification, oxidation behaviour and mechanical properties were investigated.

2. Experiment

2.1. *Powder processing*

The precursor powder were Hf (purity 99.5%, particle size — 325 mesh, Sigma–Aldrich, USA), B_4C (Grade HS, particle size ∼0.8 μm, H. C. Stack, Germany) and Si (purity 99%, particle size — 325 mesh, Sigma–Aldrich, USA). The chemical reaction can be expressed by the following equation to prepare HfB_2–SiC composite:

$$2Hf + B_4C + Si \rightarrow 2HfB_2 + SiC. \quad (1)$$

The volume contents of HfB_2–SiC composite were 74.08 and 25.92 vol.%. The theoretical density of the composite with respect to the rule of mixture is 9.14 g/cm^3. Two milling methods were adopted, in which one to mix and another to reduce the particle size of the precursor powders. In the first method, the precursor powder was ball-milled in ethanol for 24 h using ZrO_2 as a milling media and designated as HS. In another method, the precursor powder was vibration milled using ZrO_2 as a milling media in a Teflon jar for 2 h to reduce the particle size of the powders and designated as MHS. To investigate the optimum reaction and sintering conditions of the HfB_2–SiC composite with high densification at a low temperature, pressureless heat treatment was conducted. The powder sample was pressed into disc-shaped pellet followed by cold isostatic pressure (CIP) under 200 MPa and heat-treated in the temperature range of 800–1800°C for 1 h under an Ar atmosphere with a heating rate of 10°C/min. From the above basic experimental condition the composites were sintered using the reactive hot pressing at different temperatures of 1800 and 1900°C for 1 h under pressure of 32 MPa in an Ar atmosphere.

The relative bulk density was measured using the Archimedes methods, and phase composition was determined by an X-ray diffractometer (XRD, Rigaku, D/MAX-IIIC X-ray diffractometer, Tokyo, Japan), CuKα radiation (λ = 0.15406 nm at 40 kV and 45 mA). The microstructure of reacted powder mixture and sintered pellets were examined by a scanning electron microscopy (FE-SEM Philips XL30 FEG, Eindhoven, the Netherlands) and a software program(ImageJ). The polished samples were subjected to the oxidation test under air atmosphere. Each specimen was heat treated at 1500°C for 30 min in a tube furnace with a heating rate of 5°C/min. Hardness and fracture toughness of the samples were determined using Vickers indentation at a load of 2 kg and a dwell time of 15 s. The fracture toughness was estimated through the following equation:

$$K_{IC} = 0.0319 \frac{P}{al^{1/2}}$$

where P is the applied load, a the mean indentation half-diagonal length, and l is the crack length. A flexural strength was measured by three point bending method.

3. Results and Discussion

3.1. *The powder synthesis via solid-state precursors*

Figure 1 shows the XRD patterns of pressureless heat-treated HfB_2–SiC composite at different temperatures. The patterns revealed that there was no apparent change in the reaction powder mixture even after heat treated to 800°C for 1 h. The samples heat treated at 1000°C revealed the formation of a cubic phase HfC, in addition with Si and Hf peaks, which indicates the reaction between Hf and B_4C occurs at 1000°C. This phenomenon can be explained by conventional reactive hot press model.[10,11] At a suitable reaction temperature, it is assumed that B and C

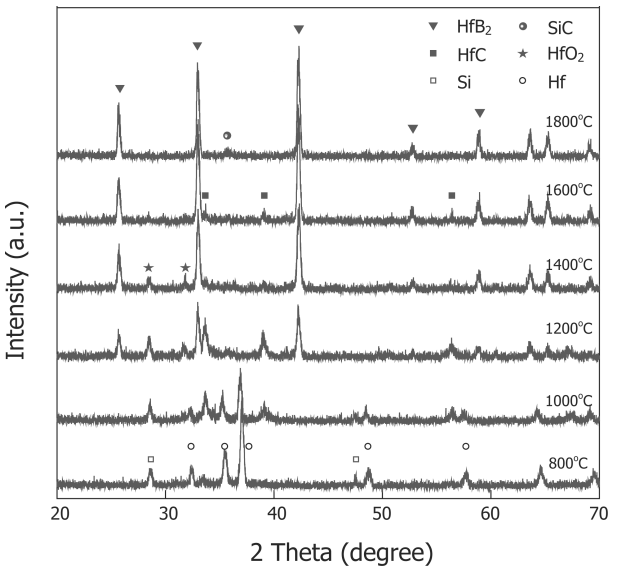

Fig. 1. The XRD patterns of the Hf/B_4C/Si mixed powders which are heat-treated at different temperatures for 60 min in Ar.

atoms from B_4C diffuse faster than Hf and Si. Among this the diffusion rate of C is higher than that of B, and easily reacts with Hf as Si possesses lower chemical reactivity than Hf. As a result, it is evident that formation of HfC occurs at lower temperature 1000°C and faster than HfB_2 and SiC. Thus, it can be concluded that HfB_2 formation required a higher temperature compared with HfC. The formation of HfB_2 occurs at a relatively higher temperature above 1200°C by a reaction between Hf and B or residual B_4C due to the increment of the diffusion rate of B. By analyzing the reaction sequence, it can be evidently concluded that the reactions (2) and (3) may occur in two steps as follows:

$$\mathrm{Hf} + \mathrm{B_4C} \rightarrow \mathrm{HfC} + 4\mathrm{B} \tag{2}$$

$$2\mathrm{Hf} + 4\mathrm{B} \rightarrow 2\mathrm{HfB_2}. \tag{3}$$

The above reactions (2) and (3) possess negative Gibbs free energies of $\Delta G_{1000} = -126$ and $\Delta G_{1000} = -630\,\mathrm{kJ/mol}$, respectively, indicating that the reactions are all thermodynamically favorable. In the XRD patterns, it is observed that the sample heat treated at 1200°C revealed the formation of HfO_2 phase. The presence of HfO_2 might be attributed to oxide impurities in the precursor powder and/or oxygen uptake during milling process. Further increase in reaction temperature result in the formation of HfB_2 as the main phase and the intensity of HfC continues to decrease based on the peak intensity in Fig. 1. At high temperatures, HfC was unstable in the presence of B_4C and Si according to reaction (4) and as discussed above, HfC was formed by the reaction between Hf and B_4C, and was later consumed in reaction (4):

$$2\mathrm{HfC} + \mathrm{B_4C} + 3\mathrm{Si} \rightarrow 2\mathrm{HfB_2} + 3\mathrm{SiC}. \tag{4}$$

Reaction (4) is also exothermic and also thermodynamically favorable even at 1000°C. The appearance of low intensity XRD peaks at 35.65° indicates that the formation of SiC occurs near the 1600°C, which is higher than HfB_2 and HfC because of low reactivity of Si. The XRD pattern of sample reacted at 1800°C showed formation of final composite HfB_2, SiC without any secondary phase. As a result, it can be concluded that the overall powder reaction takes place in two steps, in which the initial reaction initiated the formation of HfC and at higher temperatures, simultaneous reactions take place by reactions (3) and (4) and formed HfB_2, SiC and elimination of HfC. Similar steps were followed for the vibration milled powder MHS to obtain HfB_2–SiC composite. During the milling process 1.5 wt.% of ZrO_2 impurity was introduced because of wear of the ZrO_2 balls. ZrO_2 impurity can be removed by B_4C following reaction (5):

$$5\mathrm{B_4C} + 7\mathrm{ZrO_2} \rightarrow 7\mathrm{ZrB_2} + 5\mathrm{CO}\ (\mathrm{g}) + 3\mathrm{B_2O3}\ (\mathrm{l}). \tag{5}$$

Reaction (5) is well defined in the previous report.[6] Reaction between B_4C and ZrO_2 was initiated around 1200°C and complete reaction occurred at 1450°C to form ZrB_2. In literature, there are reports on the mutual continuous solid solution forms among Groups IV and V of dibiride,[12] i.e. ZrB_2 could form continuous solid solution with HfB_2. Thus, ZrO_2 contamination from ZrO_2 balls was accommodated in the HfB_2 lattice by the formation of solid solution via additional B_4C at the stoichiometric of reaction (5). In case of MHS, it was observed from the XRD pattern that there was negligible peak shift (not shown here); this may be due to a small amount of ZrO_2 contaminations. The reaction sequence was similar with HS except for the initiation temperature of reaction between Hf and B_4C and formation of HfB_2 were decreased to 800 and 1000°C, respectively. Particle size reduction via vibration milling provides the

shorter diffusion path and this might decrease the reaction temperature.

3.2. *Microstructure*

SEM analysis was conducted to investigate particle size and morphology of HS and MHS after the completion of the reaction. Figure 2(a) shows the fracture surface of HS after reaction at 1800°C, and Fig. 3(a) shows the microstructure of HS densified at 1900°C for 60 min. After the reaction at 1800°C, HS consists of large particles up to 40 μm that contains sub-micron meter grains and randomly distributed

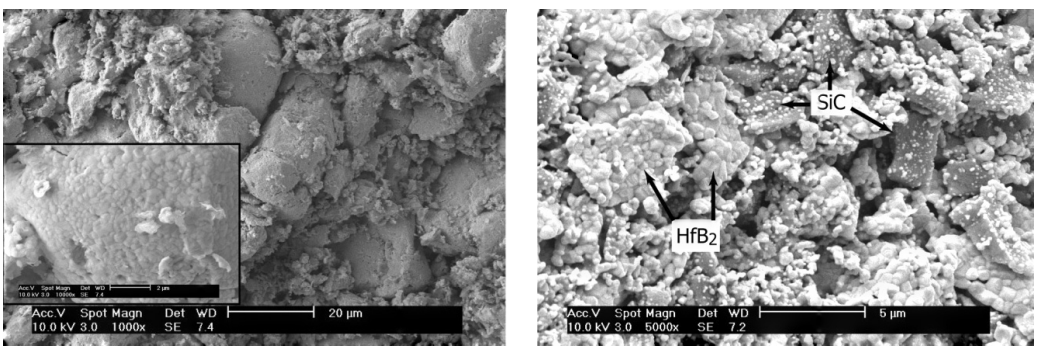

(a) (b)

Fig. 2. SEM images of the fracture after heat-treated at 1800°C for 60 min (a) HS, and (b) MHS.

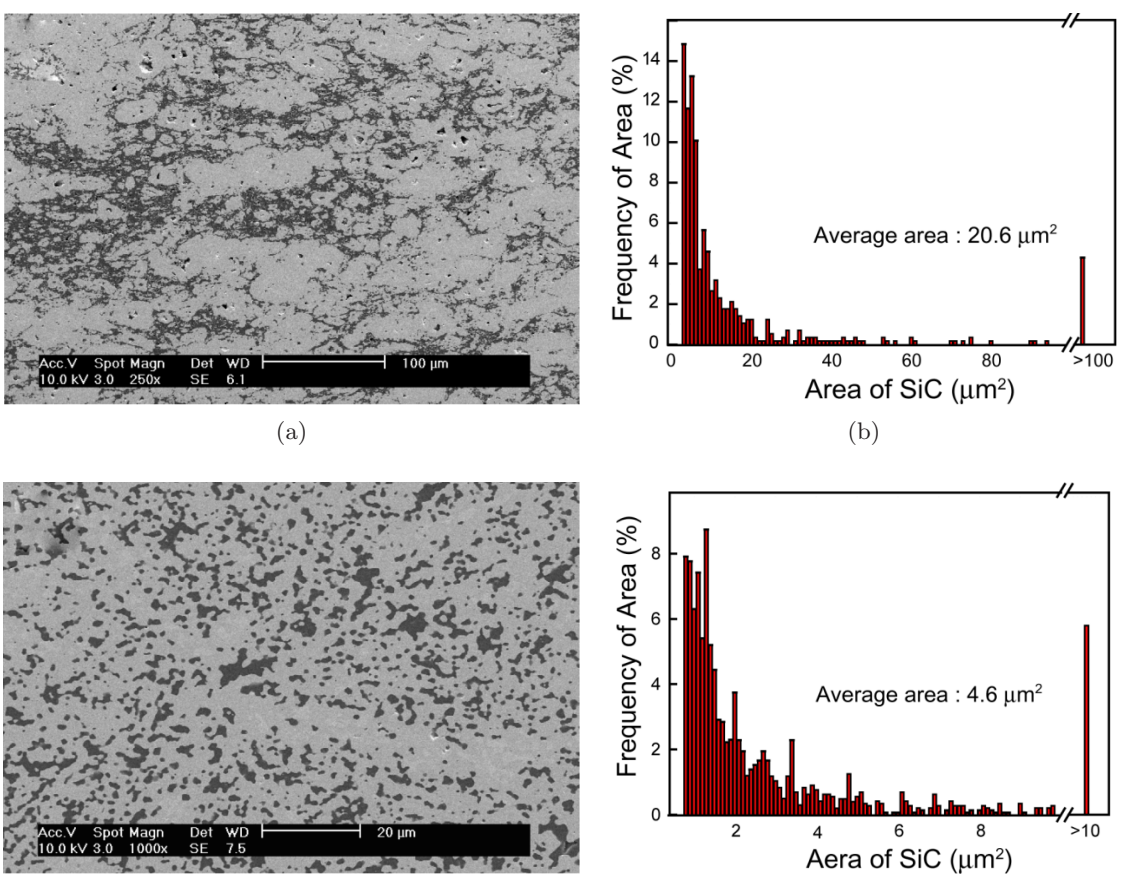

(a) (b)

(c) (d)

Fig. 3. SEM micrographs of polished surface and area of SiC phase of sample HS (a), (b) and sample MHS (c), (d).

particles. This result can be correlated with the chemical reaction at 1800°C yield HfB_2 and SiC and the large grains might be HfB_2, and the others are HfB_2 and SiC. As discussed above, during the reaction process, the diffusion rates of Hf and Si atoms are slow and the compound formation is mainly controlled based on the reactivity and diffusion rates of boron and carbon. Due to the large particle size of the Hf precursor powder and the resultant product HfB_2 also formed with similar size grains, in the RHPed composite as shown in Fig. 3(a). Thus, as shown in Fig. 3(a), microstructure is inhomogeneous with large HfB_2 (light phase) grains and non-uniform distribution of SiC (dark phase). Size and morphology of formed HfB_2 and SiC are related to its original particle size and shape. Although as shown in Fig. 2(a) inset, primary grain of formed HfB_2 is sub-micron meter size, the sizes of the secondary HfB_2 grains are larger. This large grain might be the formation of residual porosity and, therefore, limit the final densities (96.3% R.D.). The size and morphology of MHS after reaction at 1800°C for 1 h is shown in Fig. 2(b). It can be observed in the Fig. 2(b), the particle size of formed HfB_2 is about 5 μm and also consists of sub-micron size primary grains and about 3 μm SiC. The polished surface of RHPed MHS is shown in Fig. 3(c). The pellets sintered via RHP at 1900°C revealed complete densification (99.8% R.D.) with rare residual pores and homogeneous microstructure with uniform distribution of SiC. As shown in Fig. 3(d), average area of the SiC particulate is also reduced in MHS (4.6 μm^2) compared with HS (20.6 μm^2). And this area size reduction of SiC also means microstructure of MHS is more homogeneous than HS with well distributed SiC in HfB_2 matrix. From this analysis, it can be concluded that the particle size reduction via vibration milling can obtain small size HfB_2 compared with as-received powder. Increased driving force due to the formation of small size of HfB_2 and application of external pressure during the RHP process led to the nearly high densification without residual pore. In addition to the formation of small particles, increase in the defect concentration owing to the high milling also could possibly be a reason for the increased densification behaviors similar to the study of particle size effects on the sintering of boride compound.[13]

3.3. *Oxidation behavior*

Figure 4 shows the cross-sectional analysis of the oxidized HS and MHS samples heated in air at 1500°C for 30 min. The oxidation behaviors of the two samples appear to be similar, except for the distribution of surface SiO_2 layers. Oxidation of MHS produced a structure that consisted of three layers. As shown Fig. 4(b), oxidized cross-section consists of SiO_2 (~3 μm), SiC-depleted layer (~10 μm) and un-reacted HfB_2–SiC layer. The formation of layered structure is consistent with observations of other investigators who have studied ZrB_2–SiC and HfB_2–SiC.[3,4,14] But in case of HS, distribution of the SiO_2 layer on the surface was non-uniform over the

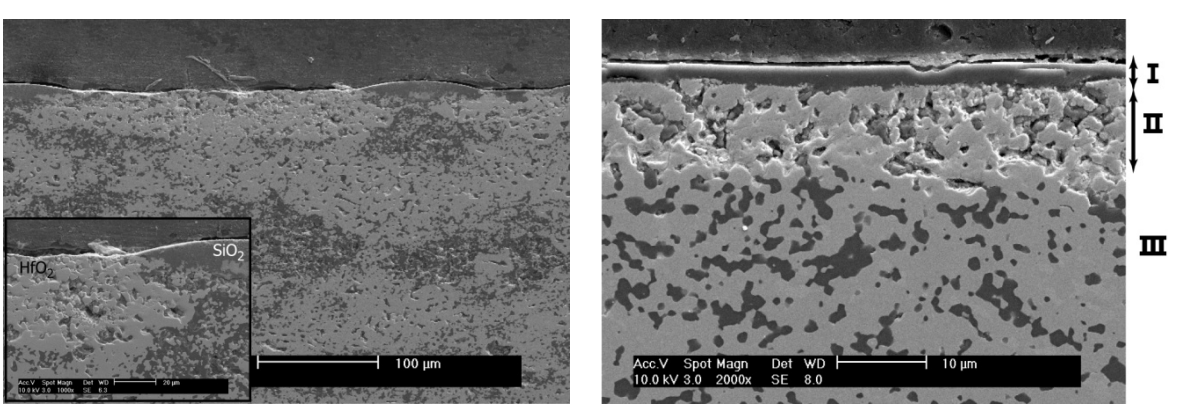

(a) (b)

Fig. 4. SEM images of (a) HS showing non-uniform SiO_2 distribution, and (b) MHS showing a uniform layer of SiO_2 (I), SiC depleted layer (II), and un-reacted HfB_2–SiC layer (III) after exposure of samples at 1500°C for 30 min in air.

specimen surface. This might be due to the inhomogeneous microstructure which is originated from large starting Hf powder. In the HfB_2 rich region, there was no Si source. Thus, monolithic HfB_2 was exposed to the 1500°C in air. As HfB_2 is exposed to 1500°C in air, it can be possibly oxidized as following the reaction (6)

$$HfB_2 + 5/2O_2 \rightarrow HfO_2 + B_2O_3\ (l). \qquad (6)$$

In literature, there are many reports that describe the high vapour pressure of B_2O_3 at 1500°C,[14] and thus B_2O_3 will evaporate rapidly leaving a porous HfO_2. If B_2O_3 evaporates during the oxidation, as is the case for monolithic ZrB_2 (or HfB_2), the effective diffusion barrier is reduced since the porous HfO_2 layer alone does not protect the underlying HfB_2 from rapid oxidation. In this region, HfB_2 oxidation will exhibit linear kinetics, i.e. oxidation depth is increased linearly with time and reaction rate-controlled kinetics can be predicted. In contrast to locally SiC rich region, parabolic oxidation behavior like MHS was predicted by encouraging the formation of Si rich glass layer on the SiC rich region, as shown in Fig. 4(a). Nonuniform distribution of SiO_2 may be due to wetting characteristics and/or local variation such as microstructure with small effective area due to the large SiC area ($20.6\,\mu m^2$) that might enhance the local oxidation rate.

3.4. *Mechanical properties*

The relative density and mechanical properties of the composites are listed in Table 1. The variation in the flexural strength was well reflected in the change of relative density and microstructure features. The incensement of flexural strength in MHS compared with HS due to the finer raw powder via vibration and thus, higher density and lower pore distribution with well distribution of SiC phase in the bulks. The fracture toughness of MHS is slightly high compared with the HS. But fracture toughness of HS and HMS is high with the other HfB_2–SiC composite densified by hot pressing.[15] The Vickers hardness was 17.7, 17.5 and 18.3 GPa for HS1900, MHS1800 and MHS1900, respectively, showing they were in a similar level. But hardness is increased to 18.3 GPa for MHS due to the full density with no porosity compared with HS1800. Hardness has been shown to decrease exponentially as the porosity increases for ceramic materials.[16]

Table 1. Relative density and mechanical properties of the RHPed samples.

Material	Relative density (% TD)	Flexural strength (MPa)	Fracture toughness ($MPam^{1/2}$)	Vickers hardness (GPa)
HS 1800°C	89.5	297 ± 20	4.17 ± 0.38	14.2 ± 0.4
HS 1900°C	96.3	551 ± 40	4.78 ± 0.42	17.7 ± 0.5
MHS 1800°C	97.2	578 ± 23	4.87 ± 0.20	17.5 ± 0.5
MHS 1900°C	99.8	692 ± 58	5.23 ± 0.17	18.3 ± 0.3

4. Conclusions

This work reported reactive powder synthesis via solid-state precursors, microstructure, oxidation behavior and mechanical properties prepared from a mixture of $Hf/B_4C/Si$ powders. The reactions of the powder mixture commenced at 1000°C and completed at 1800°C. A relative density densified with vibration milled power mixture was 99.8% at 1900°C. The enhanced densification and uniform microstructure was attributed formation of fine HfB_2 and SiC phases. The size reduction of starting powder gave the homogeneous microstructure with uniform distribution and increased effective area of SiC which play a critical role of improving the oxidation resistance and provided uniform oxidation behavior over the whole specimen. The size reduction of starting powder also led to higher mechanical properties. The mechanical properties for the fully dense RHP materials were comparable to reported value.

Acknowledgments

This work was supported by the Agency for Defense Development under the contract UE075126GD. S. J. Lee would like to thank the National Research Foundation of Korea (NRF) grant funded by the Korea government (MEST) (No. 2008-0062204).

References

1. A. K. Kuriakose and J. L. Margrave, *J. Electrochem. Soc.* **111** (1964) 827.
2. K. Upadhya, J.-M. Yang and W. P. Hoffman, *Am. Ceram. Bull.* **58** (1997) 51.
3. A. Rezaie, W. G. Fahrenholtz and G. E. Hillmas, *J. Eur. Ceram. Soc.* **27** (2007) 2495.

4. P. Lespade, N. Richet and P. Goursat, *Acta Astronautica* **60** (2007) 858.
5. D. M. Van Wie, D. G. Drewry Jr., D. E. King and C. M. Hudson, *J. Mater. Sci.* **39** (2004) 5915.
6. S. C. Zhang, G. E. Hilmas and W. G. Fahrenholtz, *J. Am. Ceram. Soc.* **89** (2006) 1544.
7. S. C. Zhang, G. E. Hilmas and W. G. Fahrenholtz, *J. Am. Ceram. Soc.* **91** (2008) 26.
8. L. Silvestroni and D. Sciti, *Scripta Mater.* **57** (2007) 165.
9. A. Bellosi, F. Monteverde and D. Sciti, *Int. J. Appl. Ceram. Technol.* **3** (2006) 24.
10. G.-J. Zhang, Z.-Y. Deng, N. Kondo, J.-F. Yang and T. Ohji, *J. Am. Ceram. Soc.* **83** (2000) 2330.
11. W.-W. Wu, G.-J. Zhang, Y.-M. Kan and P.-L. Wang, *J. Am. Ceram. Soc.* **89** (2006) 2967.
12. M. J. Gasch, D. T. Ellerby and S. M. Johnson, *Handbook of Ceramics Composites* (Springer, Chap. 9, 2005), p. 197.
13. B. Cech, P. Oliverus and J. Sejbal, *Powder Metall.* **8** (1965) 142.
14. W. G. Fahrenholtz, *J. Am. Ceram. Soc.* **88** (2005) 3509.
15. F. Monteverde, *J. Alloys Compd.* **428** (2007) 197.
16. V. Milman, S. I. Chugnova, I. V. Goncharova, T. Chudoba, W. Lojkowski and W. Gooch, *Int. J. Refract. Metal Hard Mater.* **17** (1999) 361.